International Conference on Space Optics—ICSO 2018

Chania, Greece

9–12 October 2018

Edited by Zoran Sodnik, Nikos Karafolas, and Bruno Cugny

On-orbit alignment and wavefront compensation of segmented aperture telescope using adaptive optics

Norihide Miyamura

International Conference on Space Optics — ICSO 2018, edited by Zoran Sodnik, Nikos Karafolas, Bruno Cugny, Proc. of SPIE Vol. 11180, 1118070 · © 2018 ESA and CNES · CCC code: 0277-786X/18/$18 · doi: 10.1117/12.2536171

On-orbit alignment and wavefront compensation of segmented aperture telescope using adaptive optics

Norihide Miyamura*[a]
[a]Meisei University, 2-1-1 Hodokubo, Hino, Tokyo, JAPAN 191-8506

ABSTRACT

For small satellite remote sensing missions, a large aperture telescope more than 400mm is required to realize less than 1m GSD observations. However, it is difficult or expensive to realize the large aperture telescope using monolithic primary mirror with high surface accuracy. A segmented mirror telescope should be studied especially for small satellite missions. We describe the conceptual design of the optical system that involve the segmented primary mirror and adaptive optics system, then we show numerical simulation results of the optical performance.

Keywords: Earth observation, Remote sensing, Small satellite, Phase diversity, Adaptive optics

1. INTRODUCTION

High resolution earth observation using small satellites is required. For improving the resolution of the optical system and improving the S/N, it is necessary to increase the aperture, and in advanced missions a telescope with a primary mirror diameter of several meters is required. In the space telescope, a reflection optical system is often used, but there is a limit in terms of manufacturing and cost to increase the aperture with a single primary mirror. A segmented mirrors telescope using several mirrors have been studied to realize a larger aperture[1-4].

On the other hand, space optical systems are exposed to the harsh conditions compared to ground telescopes, such as the vibration environment at launch and the thermal environment in space. As a result, misalignment, thermal deformation occurs in an optical element such as a mirror, and the performance of the optical system deteriorates. In the space optical system, since it is difficult to readjust the degradation factors unlike the ground systems, the structure is designed to keep the distortion within an allowable range, which is one cause of the mass increase.

In this research, we construct an mathematical simulation model using a segment telescope and examine the optical performance when a misalignment due to parallel movement and rotation occurs in segment mirrors. Moreover, by integrating the compensating optical system using a deformable mirror which can deform the shape of the surface with an actuator and the phase diversity method[5], we propose a method to estimate the wavefront aberration. We show that the image quality obtained by the image sensor improves using the deformable mirror.

2. SEGMENTED APERTURE TELESCOPE

The optical layout and ray tracing results of the segment telescope in this study are shown in Fig. 1. Light incident from the light source placed at the left side of the figure enters the segment mirror M1, and is imaged by the image sensor via M2, M3, DM, and M4. Here, M2, M3, and M4 are reflecting mirrors, and DM is a deformable mirror. In M3, divergent light is converted into parallel light and guided to DM. The DM adds modulation to the wavefront and corrects wavefront aberration.

In the case of diagonal line of one segment mirror is 300 mm, the diameter of the primary mirror is 813 mm. The diameter of the inscribed circle is 300 mm, and the focal length is 7.4 m.

The point spread function (PSF) of the segment telescope is shown in Fig. 3, and the modulation transfer function (MTF) is shown in Fig. 4.

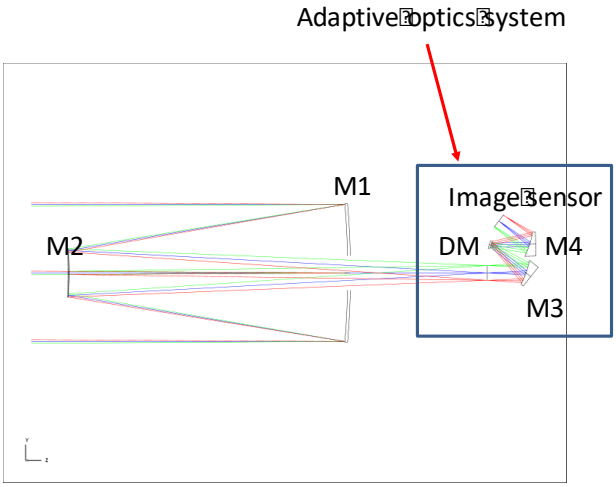

Figure 1. Optical ray out of the segmented mirrors telescope.

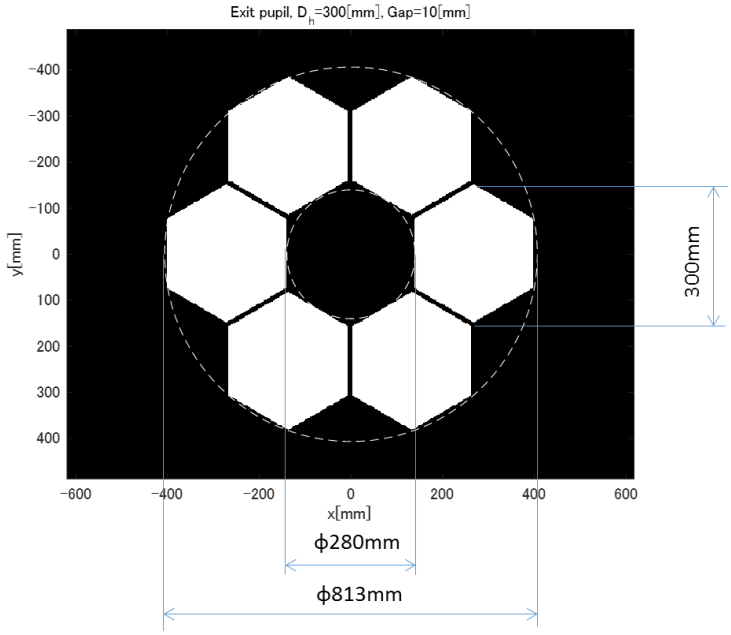

Figure 2. The primary mirror constructed by six hexiagonal segment mirrors.

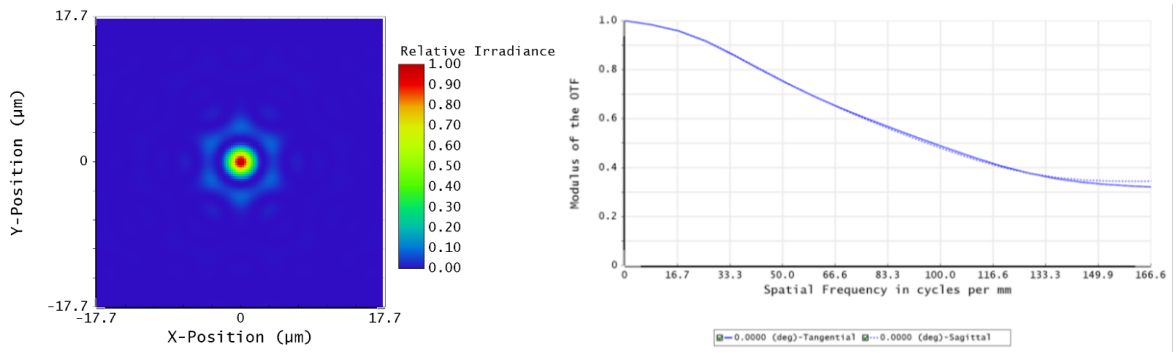

Figure 3. A point spread function (left) and a modulation transfer function (right) of the segmented mirrors telescope.

3. OPTICAL PERFORMANCE DUE TO MISALIGNMENTS OF SEGMENT MIRRORS

As shown in Fig. 4, a Z axis is taken in the optical axis direction and an X-Y plane is taken perpendicular to the optical axis. We examined the influence of the rotation of each segment mirror about the X axis and Y axis and the parallel movement in the Z axis direction on the optical performance. Here, the Strehl ratio was used to evaluate the performance of the optical system.

A random misalignment of 3 degrees of freedom was given for each mirror so that the peak to valley of the wavefront aberration was a specific value between 0.2 m and 0.3 m. Next, The PSF was calculated, and the ratio of the maximum value of PSF to the maximum value of PSF of aberration-free optical system was taken as Strehl ratio. These calculations were performed 100 times for each PV value and the distribution of the Strehl ratio was examined and the results are shown in Fig. 5. According to this result, when the PV is 0.2 µm , the Strehl ratio of approximately 0.8 is realized. However, the Strehl ratio decreases as the PV increases. As an example, calculation results of the wavefront, the PSF, and the image when PV is 0.2 µm and 0.8 µm are shown in Fig. 3 and Fig. 4.

The Strehl ratio when PV is 0.2 µm is 0.79, and it is difficult to understand clear image quality degradation only with images. On the other hand, when the PV is 0.8 µm , the Strehl ratio drops to 0.27, and apparently the image quality is degraded. According to the calculation result of the PSF, it can be seen that the point image appears at different positions due to the inclination of the segment mirror.

Therefore, if misalignment errors can be distributed so that the total wavefront PV is less than 0.2 µm , readjustment on orbit is not necessary. However, when the PV of the wavefront is larger than 0.2 µm , some correction on the orbit is necessary.

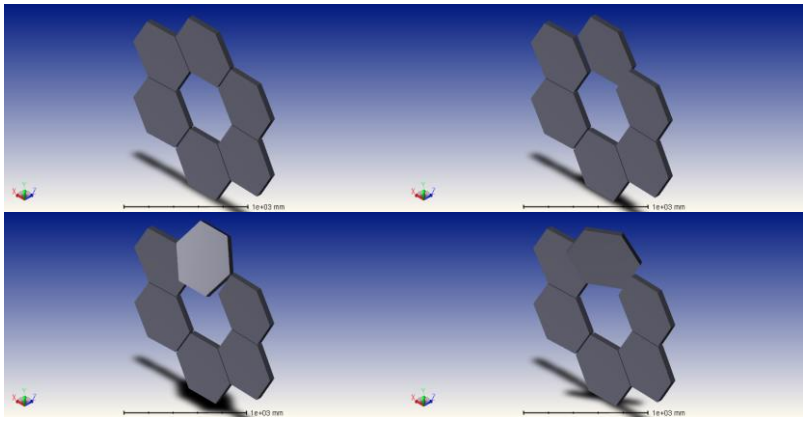

Figure 4. Misalignments of segment mirrors in 3 degree of freedom.

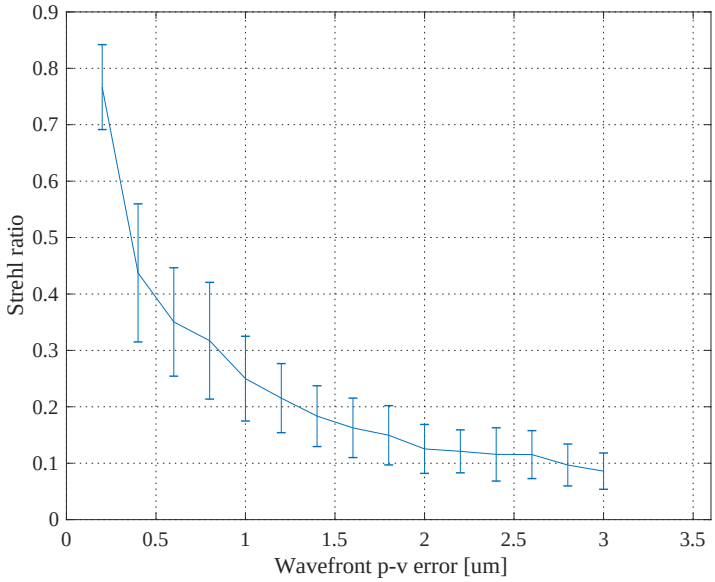

Figure 5. Relationship between wavefront error due to misalignments and the Strehl ratio.

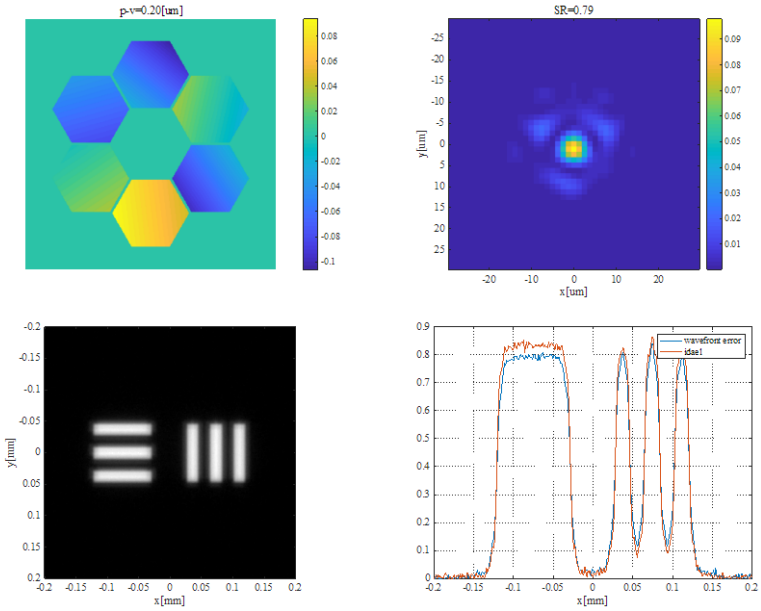

Figure 6. Optical performance due to misalignments of segment mirrors, PV=0.20 [μm], wavefront (upper left), PSF (upper right), observed image (lower left), and pixel values of the image (lower right).

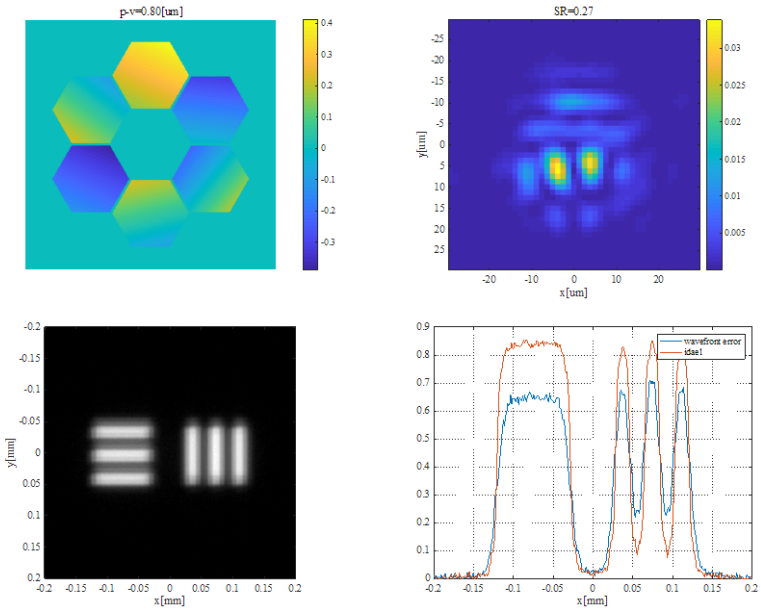

Figure 7. Optical performance due to misalignments of segment mirrors, PV=0.80 [μm], wavefront (upper left), PSF (upper right), observed image (lower left), and pixel values of the image (lower right).

4. ABERRATION ESTIMATION USING DEFORMABLE MIRROR

According to Fourier optical theory[6], observation images are represented by Eq. (1), using the PSF of the optical system $s(\boldsymbol{r}_i)$, observation target $o(\boldsymbol{r}_i)$, and observation noise $n(\boldsymbol{r}_i)$. Here, $\boldsymbol{r}_i = (x_i, y_i)$ represents a position vector on the image plane. The PSF representing the characteristics of the optical system is obtained based on the Fourier transform of the generalized pupil function $P_g(\boldsymbol{r}_p)$ of the optical system as shown in the Eqs. (2) and (3). Here, A is a constant, and λ is the wavelength of light, and z_i is the focal length. The position vector on the pupil plane is represented as $\boldsymbol{r}_p = (x_p, y_p)$. Furthermore, $P_g(\boldsymbol{r}_p)$ is expressed as shown in Eq. (4) using the pupil function $P(\boldsymbol{r}_p)$ and the wavefront function $\Phi(\boldsymbol{r}_p)$. The phase diversity method estimates unknown wavefront aberration based on this mathematical model.

$$i(\boldsymbol{r}_i) = s(\boldsymbol{r}_i) * o(\boldsymbol{r}_i) + n(\boldsymbol{r}_i) \tag{1}$$

$$s(\boldsymbol{r}_i) = \left| h(\boldsymbol{r}_i) \right|^2 \tag{2}$$

$$h(\boldsymbol{r}_i) = \frac{A}{\lambda z_i} \int \int_{-\infty}^{\infty} P_g(u,v) \exp\left(-i \frac{2\pi}{\lambda z_i} (x_i v + y_i u) \right) du dv \tag{3}$$

$$P_g(\boldsymbol{r}_p) = P(\boldsymbol{r}_p) \exp\{ i \Phi(\boldsymbol{r}_p) \} \tag{4}$$

The unknown wavefront aberration $\Phi_a(\boldsymbol{r}_p)$ is formulated as shown in Eq. (5) using the Zernike polynomials[7],

$$\Phi_a(\boldsymbol{r}_i) = \sum_{i=1}^{N} a_i Z_i \left(\frac{r_p}{\frac{D}{2}} \right) + \sum_{k=1}^{M} \sum_{j=1}^{N_s} c_{kj} \mathrm{hex}(\mathrm{r}_p - r_{ck}, D_s) Z_j \left(\frac{r_p - r_{ck}}{\frac{D_s}{2}} \right), \tag{5}$$

where, $\{a_i\}$ is Zernike coefficients of the aberration with respect to the primary mirror, D is the diameter of the primary mirror, $\{c_{kj}\}$ is the Zernike coefficients of the aberration for each segment mirror, D_s is the diagonal of the segment mirror, $\boldsymbol{r}_{ck} = (x_{ck}, y_{ck})$ is the position vector of the center of the k^{th} segment mirror , $\text{hex}(\boldsymbol{r}, D)$ is a function that becomes 1 inside a regular hexagon whose diagonal length is D and becomes 0 otherwise.

In this research, it is assumed that the entire primary mirror is projected on a deformable mirror to correct the wavefront aberration.

Using the optical wavefront $\Phi_{DM}(\boldsymbol{r}_p)$ due to the deformable mirror, the wavefront function $\Phi(\boldsymbol{r}_p)$ is expressed as shown in Eq. (6),

$$\Phi(\boldsymbol{r}_p) = \Phi_a(\boldsymbol{r}_p) + \Phi_{DM}(\boldsymbol{r}_p). \tag{6}$$

In estimating the unknown wavefront aberration, known information is given to the optical wavefront using a deformable mirror, and images are acquired. Then, the estimation of the wavefront aberration is formulated as an inverse problem of finding aberration parameters from images.

The wavefront by the deformable mirror is formulated using the known coefficient vector $\boldsymbol{b} = \{b_j\}$ and the Zernike polynomials as follows,

$$\Phi_{DM}(\boldsymbol{r}_p) = \sum_{j=1}^{J} b_j Z_j(\boldsymbol{r}_p). \tag{7}$$

In aberration estimation by the phase diversity method, it is assumed that unknown wavefront aberration is modeled by the following equation and higher order aberrations are expressed by Zernike coefficient vector $\hat{\boldsymbol{a}} = \{\hat{a}_j\}$.

$$\hat{\Phi}_a(\boldsymbol{r}_p) = \sum_{j=1}^{J} \hat{a}_j Z_j(\boldsymbol{r}_p). \tag{8}$$

Using the estimated value of the wavefront aberration $\hat{\Phi}_a(\boldsymbol{r}_p)$ and the wavefront due to the deformable mirror $\Phi_{DM}(\boldsymbol{r}_p)$, the synthetic wavefront $\Phi(\boldsymbol{r}_p)$ is considered as $\Phi(\boldsymbol{r}_p) = \hat{\Phi}_a(\boldsymbol{r}_p) + \Phi_{DM}(\boldsymbol{r}_p)$. When estimating the wavefront aberration by the phase diversity method, first, the image i_1 is acquired with DM as a flat. Next, the image i_2 is observed when aberration $\Phi_{DM}(\boldsymbol{r}_p)$ is applied using a deformable mirror. Further, the evaluation function J_D is calculated according to Eq. (9),

$$J_D = \sum_{f_x} \sum_{f_y} \frac{\left| \sum_{k=1}^{K} I_k(f_x, f_y) S_k^*(f_x, f_y) \right|^2}{\sum_{k=1}^{K} \left| S_k(f_x, f_y) \right|^2}. \tag{9}$$

By minimizing J_D with the vector $\hat{\boldsymbol{a}} = \{\hat{a}_j\}$ as a variable, the estimated value of $\hat{\Phi}_a(\boldsymbol{r}_p)$ is obtained.

5. CALCULATION RESULT OF WAVEFRONT ABERRATION ESTIMATION BY DEFORMABLE MIRROR

Based on the aberration model of Eq. (5), angle errors around the X axis and the Y axis, and parallel shift errors in the optical axis direction were randomly applied to the six segment mirrors, respectively. In addition, defocus and astigmatism of the whole optical system were applied. The PV value of the unknown wavefront aberration was set to 0.52 μm , and $\hat{\boldsymbol{a}} = \{\hat{a}_j\}$ was estimated for $J = 20$. The calculation results are shown in the Fig. 8. According to the

results, the value of the PV of the wavefront aberration is reduced from 0.52 μm to 0.33 μm although high-order term remains by wavefront compensation. Next, the images in observing the test chart are shown in the Fig. 9. Improvement in image quality due to correction of low order aberrations is confirmed.

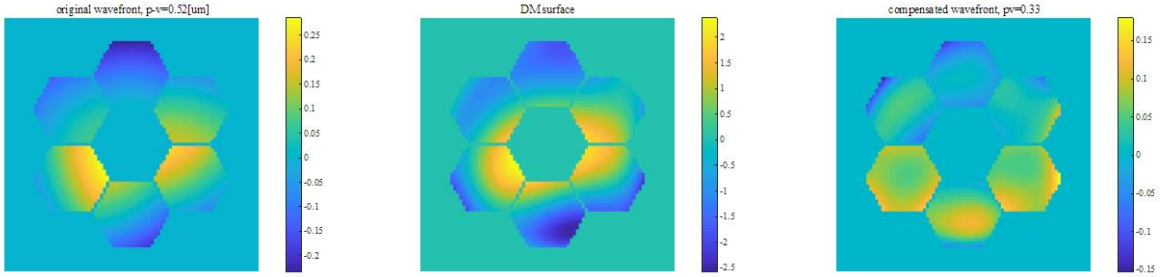

Figure 8. A wavefront aberration due to misalignments of segmented mirrors (left), a wavefront modulated by the deformable mirror (center), a compensated wavefront using deformable mirror (right).

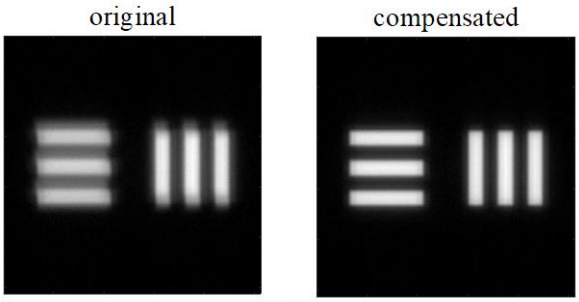

Figure 9. Numerical simulation results of the images observing the test chart

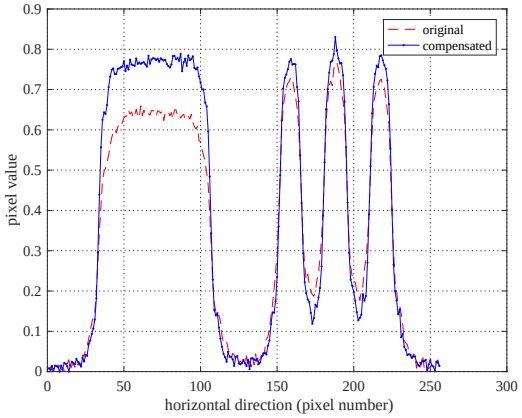

Figure 10. Pixel values of the test chart images.

6. CONCLUSIONS

In this study, a numerical calculation model using a segment mirror and a deformable mirror was constructed and optical performance by numerical calculation was investigated. Especially the optical performance in the case where the alignment error occurs in the segment mirror was studied. Furthermore, we proposed application of phase diversity method using deformable mirror, estimates wavefront aberrations, and show that image quality improves by correction using the deformable mirror.

REFERENCES

[1] Craig Underwood, Using cubesat/micro-satellite technology to demonstrate the autonomous assembly of a reconfigurable space telescope (AAReST), IAC-14.B4.2.4
[2] Craig Underwood, Sergio Pellegrino, Autonomous Assembly of a Reconfigurable Space Telescope (AAReST) - A CubeSat/Microsatellite Based Technology Demonstrator, 27th Anual AIAA/USU Conference on Small Satellite
[3] T. L. Whitman, C. Wells, J. B. Hadaway, J. S. Knight, and S. Lunt, "Alignment test results of the JWST Pathfinder Telescope mirrors in the cryogenic environment," in *SPIE Astronomical Telescopes+ Instrumentation* (2016), p. 990449.
[4] A. R. Contos, D. S. Acton, P. D. Atcheson, A. A. Barto, P. A. Lightsey, and D. M. Shields, "Aligning and maintaining the optics for the James Webb Space Telescope (JWST) on-orbit: the wavefront sensing and control concept of operations," Proc. SPIE 6265, 62650X–62650X–16 (2006).
[5] R. G. Paxman, T. J. Schulz, and J. R. Fienup, "Joint estimation of object and aberrations by using phase diversity," J. Opt. Soc. Am. A, vol. 9, no. 7, pp. 1072–1085, Jul. 1992.
[6] J. W. Goodman, Introduction to Fourier Optics 3rd edition, 3rd ed. Roberts and Company, 2005.
[7] R. J. Noll, "Zernike polynomials and atmospheric turbulence," J. Opt. Soc. Am., vol. 66, no. 3, pp. 207–211, 1976